

# Spectral Separation Resolves Partial Volume Effect in MRSI

Yuzhuo Su<sup>1</sup>, Sunitha Thakur<sup>2</sup>, Wei Huang<sup>2</sup>, Shuyan Du<sup>3</sup>, Paul Sajda<sup>3</sup>, Lucas C. Parra<sup>1</sup>

<sup>1</sup>Biomedical Engineering Department, City College of New York, Program in Engineering, the Graduate Center, City University of New York; <sup>2</sup>Neuroradiology, Memorial Sloan-Kettering Cancer Center; <sup>3</sup>Department of Biomedical Engineering, Columbia University

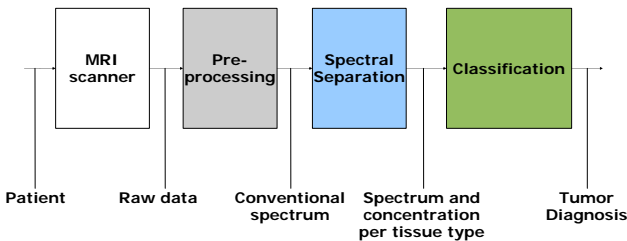
## Introduction

Cancerous tissue exhibits altered metabolite concentrations as compared to normal brain tissue. Magnetic resonance spectroscopy imaging (MRSI) reveals such abnormalities in altered spectral profiles.

Although the relations between spectral profiles and histological findings are well established, the significant variability of *in vivo* spectra, which is due to the heterogeneity of tumor tissues, large voxel sizes, and the mixture of normal brain tissues with infiltrative tumors (partial volume effect), often limits their diagnostic potential. This variability complicates tumor diagnosis and grading, as well as the determination of tumor spatial extent. Different spectral analysis methods are being developed to address this problem.

Previously we proposed an algorithm called constrained non-negative matrix factorization [1] that extracts constituent spectra associated with different tissue types by simultaneously analyzing all voxel spectra. In principle this method solves the partial volume effect as it determines also the proportion with which each constituent spectrum contributes to an individual voxel spectrum. The algorithm was shown to extract spectral profiles and their spatial distributions consistent with normal and cancerous tissue. Here we present results on 10 clinical MRSI scans of various brain tumor types and demonstrate the reduced variability of normal brain tissue across subjects.

## Strategy



•The raw data from 10 patients with brain tumor is provided by Memorial Sloan-Kettering Cancer Center.

•Preprocessing, which includes water suppression, phase corrections, and frequency alignment etc., produces conventional spectrum.

•Spectral separation is used to reduce the variability of MRSI spectra and to obtain a more consistent relation between spectral profiles and tumor type and grade.

•A pattern recognition tool that classifies the extracted spectral profiles into tumor types and grades for a given patient population as an automated aid for tumor diagnosis is being developed.

## Spectral Separation

Spectral profiles are variable due to the heterogeneity of tumor tissue, large voxel sizes, and the mixture of normal brain tissue with infiltrative tumors. The variability complicates tumor diagnosis and grading, as well as the determination of tumor spatial extent. A typical MRSI voxel often contains a combination of different tissue types, such as normal brain tissue, necrotic and cystic tissue, tumor tissue of different grades, etc [2,3,4]. In order to reduce the variability of MRSI spectra and obtain a more consistent relation between spectral profiles and tumor type and grade, we use a spectral separation method based on an algorithm known as non-negative matrix factorization (NMF). This algorithm represents each voxel's spectrum as a linear combination of constituent tissue types, each with a consistent spectrum across many voxels, and produce spectral images that quantify the abundance of each constituent tissue [5].

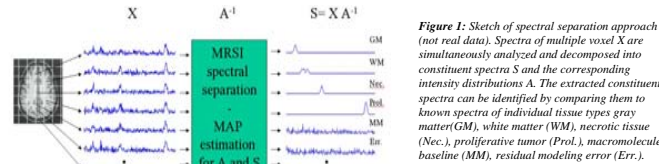


Figure 1: Sketch of spectral separation approach (not real data). Spectra of multiple voxel  $X$  are simultaneously analyzed and decomposed into constituent spectra  $S$  and the corresponding intensity distributions  $A$ . The extracted constituent spectra can be identified by comparing them to known spectra of individual tissue types gray matter (GM), white matter (WM), necrotic tissue (Nec.), proliferative tumor (Prol.), macromolecule baseline (MM), residual modeling error (Err.).

where the columns in  $A$  represent the abundance of the constituent tissue and the rows in  $S$  are the corresponding spectra.  $M$  represents additive noise. The abundance matrix  $A$  has one column for each tissue type and one row for each voxel.  $X$  and  $S$  have one column for each resonance frequency.

## Results

### Separation of long echo time <sup>1</sup>H MRSI brain spectra

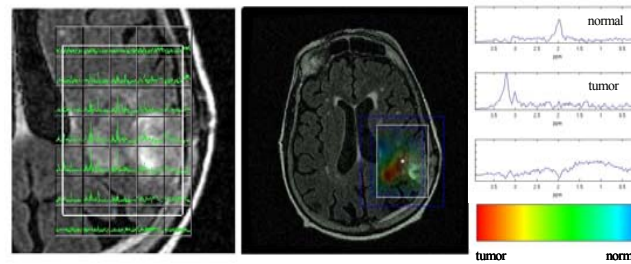


Figure 2: Comparison of conventional MRSI spectra (left) with the results of spectral separation (center, right). Left: Conventional spectra are overlaid on FLAIR image and zoomed in to show the tumor region. Center: The extracted spectral abundances – matrix  $A$  in equation (1) – are converted to a color between blue and red indicating the abundance ratio of normal and tumor spectra. This color is combined with the intensity of the FLAIR image. The white box in the two images outlines the same scan area. Left: Three spectra have been extracted. Their profile is indicative of normal tissue with high NAA content at 2ppm (top), and tumor tissue with high CHO at 3.2ppm (center). The third spectrum (bottom) captures residual baseline activity. The separation algorithm was applied to the spectrum only in the frequency range shown here. Other frequency bands contain mostly noise for these scans.

## Reduced variability on clinical <sup>1</sup>H MRSI scans

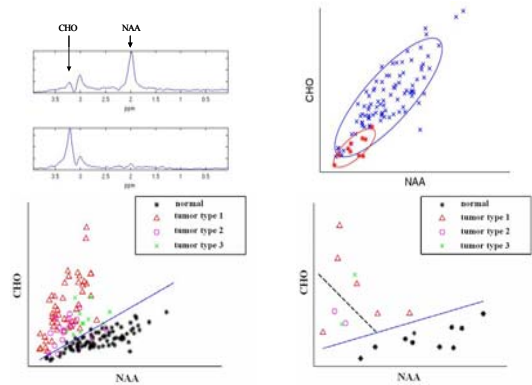


Figure 3: Effect of separation on CHO and NAA maximum peak heights. Top left: Example spectra after separation. The two spectra – shown here as example – are the result of the separation algorithm on a scan of a high grade glioma. The first spectrum corresponds to normal tissue and the second spectrum to the glioma. The arrows indicate the location where CHO and NAA maximum peak heights were measured. Top right: Reduced variability after spectral separation. The NAA and CHO peak heights define a point in this scatter plot, each point corresponding to a different spectrum. The original voxel spectra are shown in blue while the separated spectra are shown in red. All voxels included in this graph have been determined to contain only normal brain tissue. The scatter outlined by the ellipsoids indicates one standard deviation from the mean. The reduced scatter after separation is evident indicating a reduced variability. Bottom left: Illustration for classification before spectral separation. The scatter plot here also shows the peak heights of spectra corresponding to tumor tissue (colored symbols). Normal brain tissue spectra are indicated as black asterisks. The solid line dividing the two groups indicates an optimal linear classifier. Note that the standard clinical criterion of CHO/NAA concentration ratio corresponds to a line through the origin. Bottom right: Illustration for classification after spectral separation. Points indicate maximum peak heights for spectra after separation. Each of the 10 cases contributes only two points corresponding to the extracted spectrum for normal and tumor tissue. Note the reduced overlap of the tumors with normal tissue when comparing the two bottom graphs. The dashed line indicates a possible decision boundary to further differentiate between different tumor types (the red  $\Delta$  on the left of the dashed line and the green  $\times$  on the right corresponds to a scans with low SNR for which we do not obtain reliable separation).

## Conclusion and future plan

Extracted spectra and anatomical concentration distribution are consistent with classical diagnosis: tumor tissue has increased choline (CHO) and reduced NAA (N-acetyl-aspartate), which indicate that this algorithm may have potential value for diagnosis of brain tumor.

The variability of *in vivo* spectra is due to the partial volume effect, and our algorithm is effective in reducing this variability.

The next step is to develop a pattern recognition tool to extract diagnostic information from the recovered spectra and to facilitate tumor grading and classification using more metabolic parameters as well as the structure information from the MRI.

## References

- [1] Sajda P, Du S, Brown T, Stoyanova R, Shungu D, Mao X and Parra L. Nonnegative Matrix Factorization for Rapid Recovery of Constituent Spectra in Magnetic Resonance Chemical Shift Imaging of the brain. IEEE Transaction on Medical Imaging, 2004, 23.
- [2] Segebarth C, Baleriaux D, Luyten P, den Hollander J. Detection of metabolic heterogeneity of human intercranial tumors *in vivo* by <sup>1</sup>H NMR spectroscopic imaging. Magn. Resonc. Med., 1990, 13: 62-76.
- [3] Furuya S. Evaluation of metabolic heterogeneity in brain tumors using 1H-chemical shift imaging method. NMR in Biomedicine, 1997, 10: 25-30.
- [4] Fulham M. Mapping of brain tumor metabolites with proton MR spectroscopic imaging. Clinical relevance. Radiology, 1992, 185: 675-686.
- [5] Lee D and Seung H. Learning the parts of objects by non-negative matrix factorization. Nature, 1999, 401: 788–791.